Journal of Organometallic Chemistry 695 (2010) 382–391

Contents lists available at ScienceDirect

Journal of Organometallic Chemistry

journal homepage: www.elsevier.com/locate/jorganchem

Hydridic reactivity of $W(CO)(H)(NO)(PMe_3)_3$ – Dihydrogen bonding and H_2 formation with protic donors

Nataša Avramović, Jürgen Höck, Olivier Blacque, Thomas Fox, Helmut W. Schmalle, Heinz Berke *

Department of Inorganic Chemistry, University of Zürich, Winterthurerstrasse 190, 8057 Zürich, Switzerland

ARTICLE INFO

Article history:
Received 31 July 2009
Received in revised form 19 October 2009
Accepted 25 October 2009
Available online 30 October 2009

Dedicated to Prof. Ingo-Peter Lorenz on the occasion of his 65th birthday. Department of Chemistry and Biochemistry, Ludwig-Maximillians-Universität München

Keywords:
Hydrogen bonding
Dihydrogen bonding
Transition metal hydride
Tungsten
Alkoxide

ABSTRACT

The hydridic reactivity of the complex $W(CO)(H)(NO)(PMe_3)_3$ (**1**) was investigated applying a variety of protic donors. Formation of organyloxide complexes $W(CO)(NO)(PMe_3)_3(OR)$ (R = C_6H_5 (**2**), 3,4,5-$Me_3C_6H_2$ (**3**), CF_3CH_2 (**4**), $C_6H_5CH_2$ (**5**), Me (**6**) and *i*Pr (**7**)) and H_2 evolution was observed. The reactions of **1** accelerated with increasing acidity of the protic donor: Me_2CHOH (pK_a = 17) < MeOH (pK_a = 15.5) < $C_6H_5CH_2OH$ (pK_a = 15) < CF_3CH_2OH (pK_a = 12.4) < $C_6H_2Me_3OH$ (pK_a = 10.6) < C_6H_5OH (pK_a = 10).

Regioselective hydrogen bonding of **1** was probed with two of the protic donors furnishing equilibrium formation of the dihydrogen bonded complexes ROH···$HW(CO)(NO)(PMe_3)_3$ (R = 3,4,5-$Me_3C_6H_2$, **3a** and *i*Pr, **7a**) and the O_{NO} hydrogen bonded species ROH···$ONW(CO)(H)(PMe_3)_3$ (R = $C_6H_2Me_3$, **3b** and *i*Pr, **7b**) which were studied in hexane and d_8-toluene solutions using variable temperature IR and NMR spectroscopy. Quantitative IR experiments at low temperatures using 3,4,5-trimethylphenol (**TMP**) confirmed the two types of competitive equilibria: dihydrogen bonding to give **3a** ($\Delta H_1 = -5.8 \pm 0.4$ kcal/mol and $\Delta S_1 = -15.3 \pm 1.4$ e.u.) and hydrogen bonding to give 3b ($\Delta H_2 = -2.8 \pm 0.1$ kcal/mol and $\Delta S_2 = -5.8 \pm 0.3$ e.u.). Additional data for the hydrogen bonded complexes **3a,b** and **7a,b** were determined via NMR titrations in d_8-toluene from the equilibrium constants $K_{(\Delta\delta)}$ and $K_{(\Delta R_1)}$ measuring either changes in the chemical shifts of H_W ($H_{W(\Delta\delta)}$) or the excess relaxation rates of H_W (ΔR_1) (**3a,b**: $\Delta H_{(\Delta\delta)} = -0.8 \pm 0.1$ kcal/mol; $\Delta S_{(\Delta\delta)} = -1.4 \pm 0.3$ e.u. and $\Delta H_{(\Delta R_1)} = -5.8 \pm 0.4$ kcal/mol; $\Delta S_{(\Delta R_1)} = -22.9 \pm 1.9$ e.u) (**7a,b**: $\Delta H_{(\Delta\delta)} = -2.3 \pm 0.2$ kcal/mol; $\Delta S_{(\Delta\delta)} = -11.7 \pm 0.9$ e.u. and $\Delta H_{(\Delta R_1)} = -2.9 \pm 0.2$ kcal/mol; $\Delta S_{(\Delta R_1)} = -14.6 \pm 1.0$ e.u). Dihydrogen bonding distances of 1.9 Å and 2.1 Å were derived for **3a** and **7a** from the NMR excess relaxation rate measurements of H_W in d_8-toluene. An X-ray diffraction study was carried out on compound **2**.

1. Introduction

Proton transfers from protic donors to metal hydrides are thought to be preceded by hydrogen bonding, in particular dihydrogen bonding between the hydride and the protic substrate [1–31]. In conjunction with catalysis, such as "ionic hydrogenations" proceeding with proton and hydride transfers [32–37], the significance of particularly dihydrogen bonding is still a matter of dispute. Intramolecular hydrogen bonding of the hydride ligand was first discovered in the solid state in the groups of Morris and Crabtree [9–11], while the groups of Shubina and Berke provided spectroscopic, thermodynamic and structural evidence for intermolecular MH···HX bonding in solution [12–16].

Tracing intermolecular dihydrogen bonding between metal hydrides [M]–H and protic donors A–H is a difficult challenge, since the involved attractive forces are similar in magnitude to the counteracting entropy terms of the association process at room temperature. Different methods might be applied to study dihydrogen bonding of transition metal hydride complexes. The superior methodologies to examine these interactions include variable temperature (VT) IR and NMR spectroscopic studies, X-ray and neutron diffraction studies and supporting density functional theory (DFT) calculations. Crabtree's group observed intermolecular dihydrogen bonding in the crystal of the rhenium complex $ReH_5(PPh_3)_3$·indole by an X-ray diffraction study [38–41]. Based on H···H bond distances and their corresponding bond angles, the strength of the H···H bond and linearity of the H···HRe fragments could be established. In comparison to the solid state, VT IR spectroscopy carried out in solution allows observation of unique hydrogen bonded species in equilibrium. Dihydrogen bonding established with many tungsten and rhenium hydrides and acidic alcohols like phenol, hexafluoro-2-propanol (HFIP) and perfluoro-2-methyl-2-propanol (PFTB) was studied in our group using VT IR spectroscopy [12,13,27]. Various other VT IR studies showed that dihydrogen bonding species indeed precede the proton transfer processes [42–44]. Examples are the protonations of $[Re(CO)(NO)(PMe_3)_2H_2]$ [15] and $[CpRuH(CO)(PCy_3)]$ [14,45,46] with alcohols. In the latter case full protonation occurred with an

* Corresponding author. Fax: +41 1 63 56 802.
E-mail address: hberke@aci.uzh.ch (H. Berke).

0022-328X/$ - see front matter © 2009 Elsevier B.V. All rights reserved.
doi:10.1016/j.jorganchem.2009.10.036

intermediate identified as the ion pair $[CpRu(CO)(PCy_3)(\eta^2\text{-}H_2)]^+\cdots[OR]^-$. Additional stabilization originated from the contact between the dihydrogen ligand and the counter-ion. Structural elucidation of quite a few examples of these intermediates allowed for the generalization of the mechanism of the proton transfer processes under consideration [47,48,3]. NMR spectroscopic evidence for the MH···HX hydrogen bonding is acquired by upfield shifts of the hydride resonance and a decrease of the relaxation times (T_{1min}) [12]. Since such equilibrations are usually fast on the NMR time scale, respective resonances of the hydride species average and shift with the position of the equilibria. The equilibrium chemical shift $\Delta_{hydride}$, which is thus dependent on the concentrations of the hydride and the protic donor HX and on temperature, allows one to determine the equilibrium constants by curve fitting of the NMR titration. Short H···H distances, less than the sum of the van der Waals radii, were determined by NMR spectroscopy for intermolecular dihydrogen bonding in solutions of $W(CO)_2(NO)(PMe_3)_2H$ and $Re(CO)(NO)(PMe_3)_2H_2$ in the presence of the relative strongly acidic alcohol components $(CF_3)_2CHOH$ (HFIP) and $(CF_3)_3COH$ (PFTB) [13,49]. In addition to this, r(H..H) distances were also derived by measuring T_1 relaxation times for rhenium and ruthenium complexes [50,51].

In the last 15 years our group has reported the syntheses of a series of transition metal hydrides [52–80]. One of the main goals was to establish correlation between hydridicity of the hydride ligands and their activity in hydride transfers. As just derived the hydridicity of hydride ligands is one of the major parameters for dihydrogen bonding and the subsequent reaction of the protic donor with the hydrides [77–80]. Acidity and alcohol concentrations, temperature and the type of solvent played a major role in these processes [50,53,80]. We anticipated that both types of reactions might follow the same electronic principles. The tungsten hydride $W(CO)(H)(NO)(PMe_3)_3$ was studied in our group for hydride transfer reactions. Apparently due to the presence of three strong phosphine σ-donors and the nitrosyl group in *trans* position to the hydride ligand, $W(CO)(H)(NO)(PMe_3)_3$ shows a strong hydridic polarization of the M–H bond [64,78]. In support of such hydridic hydride reactions, we wanted to generate more quantitative data, which were acquired by aid of IR and VT NMR spectroscopies and in suitable cases also X-ray diffraction studies.

2. Results and discussion

2.1. Reaction of $W(CO)(H)(NO)(PMe_3)_3$ (**1**) with a variety of alcohols

It was mentioned before that the reactions of hydride complexes with protic donors to yield organyloxide complexes and H_2 presumably proceed via the intermediacy of dihydrogen bonding adducts as contact pairs (K_1). The overall reaction rates may be related to stereoelectronic influences of the protic donors via the tightness of the K_1 equilibria (adduct concentrations) and the barriers of the subsequent reactions represented by $k(H_2)$. We thought we could quantitatively probe such reactivity of **1** with phenols and alcohols of different steric bulks and acidities, such as phenol (pK_a = 10), 3,4,5-trimethylphenol (pK_a = 10.6), 2,2,2-trifluoroethanol (pK_a = 12.4), benzyl alcohol (pK_a = 15), methanol (pK_a = 15.5) and isopropanol (pK_a = 17) and look for correlation of the reactions of **1** with the alcohols and their acidities. Using quantitative ^1H and $^{31}P\{^1H\}$ NMR, such reactions were followed in toluene-d_8 at 60 °C yielding the organyloxide complexes $(ON)(OC)(Me_3P)_3W(OR)$ (R = C_6H_5 (**2**), 3,4,5-$Me_3C_6H_2$ (**3**), CH_2CF_3 (**4**), $CH_2C_6H_5$ (**5**), Me (**6**), Me_2CH (**7**)) and H_2.

The reactions were complete after approximately 4, 5, 20, 24, 24 and 72 h for phenol, 3,4,5-trimethylphenol (**TMP**), benzyl alcohol, 2,2,2-trifluoroethanol, methanol and isopropanol, respectively. For the reactions with phenol and **TMP** two equivalents were used, but in the cases of the generally less acidic aliphatic alcohols, three equivalents of the alcohols were needed to drive the reactions to completion within a reasonable span of time. Plots of the decay of **1** vs. time *t* allowed an exponentional fitting with a first order law. A mechanism could not be demonstrated from these studies nevertheless, it is clear that these reactions do not involve a rate determining bimolecular step (second order) of the hydride with the alcohols. In agreement with the evidence to be described later, we assume the involvement of dihydrogen bonding pre-equilibria and subsequent rate determining first order decays of the formed dihydrogen bonding adducts (Scheme 1). The half-life times of these reactions to **2**–**7** were 46, 57, 216, 218, 275 and 815 min. A plot of these half-life times vs. pK_a of the corresponding protic donor confirms gross dependence on the acidity of the protic donor, i.e. predominant electronic influence (Fig. 1). Steric influence was apparently prevailing in the case of the reaction of **1** with isopropanol being somewhat outside of the correlation window of the fairly linear dependence of the other protic donors of Fig. 1. Isopropanol possesses a much slower reaction rate.

The IR spectra of compounds **2**–**7** displayed ν(NO) and ν(CO) bands in the region of 1500–2000 cm^{-1}. While the ν(CO) bands of these compounds showed a quite small spread of 5 cm^{-1}, the ν(NO) bands appeared between 1584 and 1565 $cm^{-1}$and were more sensitive to the nature of their *trans* organyloxide moieties [64] showing increasing wavenumbers in the order of **7** < **6** < **5** < **4** < **3** < **2**. An almost linear regression was found for the ν(NO) bands with the pK_a of the reacting protic donors (Fig. 2) proving in this order lower basicity of the organyloxy residue.

The ^1H NMR spectra supported the structures of the organyloxide complexes further. For all compounds characteristic resonances could be attributed to the OC*H* moieties appearing as a quartet at 3.87 ppm for **4**, as singlets at 4.86 for **5** and at 3.67 for **6** and as a septet at 3.78 ppm for **7**. In addition, the $^{13}C\{^1H\}$ NMR spectra of **4**–**7** displayed characteristic signals for the O*C*H carbon atoms at 71.8, 75.8, 62.3 and 70.9 ppm and signals for the *C*O ligands at around 229 ppm. Crystals of **2** suitable for X-ray diffraction study were grown from a saturated pentane solution at −30 °C. The structure displays a tungsten center with pseudo-octahedral coordination. The nitrosyl group is located *trans* to the alkoxide ligand and the three PMe_3 ligands lie together with the CO ligand in a plane (Fig. 3).

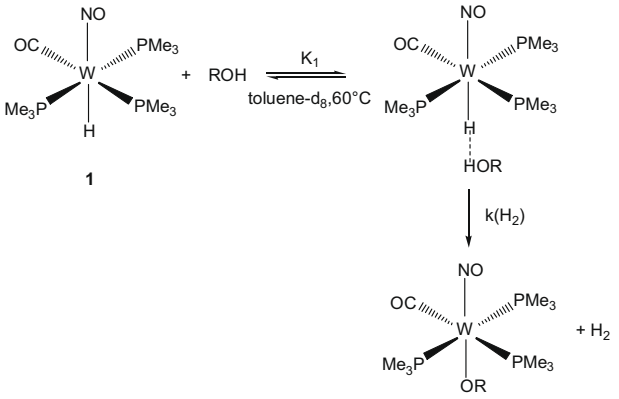

Scheme 1.

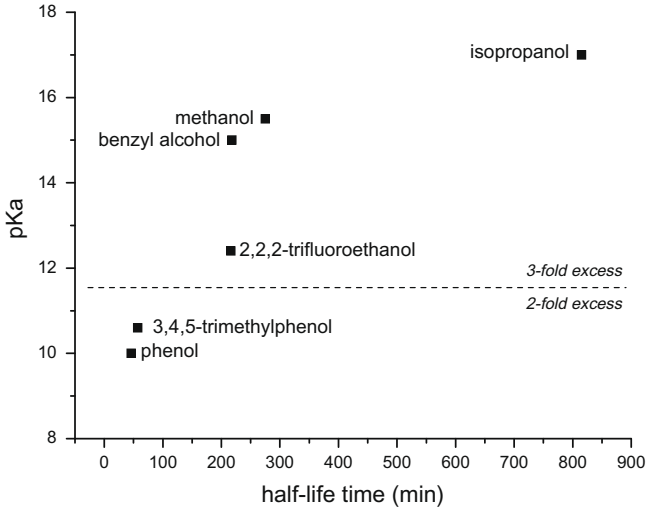

Fig. 1. Correlation plot between the half-life time of the tranformations of **1** with the indicated alcohols to give **2**–**7** and the p*K*a of the alcohols.

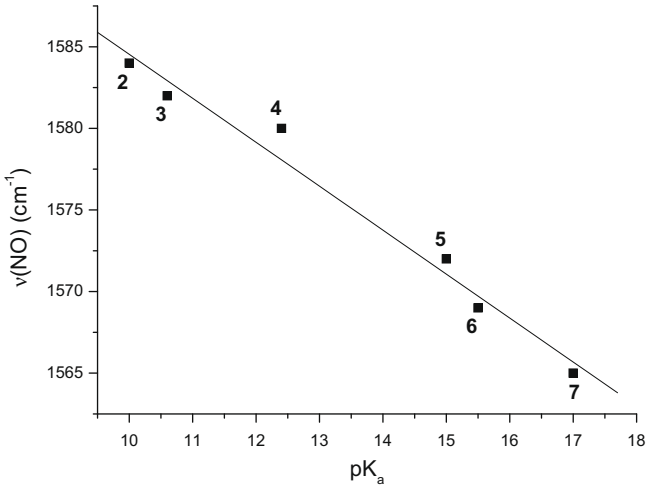

Fig. 2. Correlation between ν(NO) of the organyloxide complexes **2**–**7** (cm^{-1}) and the pK_a of their conjugate alcohols.

2.2. Hydrogen bonding of *1* with protic donors: VT IR and VT NMR studies

It was mentioned before that dihydrogen bonding adducts characterized by K_1, but also hydrogen bonding adducts to O_{NO} (K_2), may precede the formation of the organyloxy products according to Scheme 1. Therefore we found it intriguing to trace the nature of these hydrogen bonding equilibria between **1** and the protic donors by quantitative variable temperature IR and NMR methodologies [2–6,12–28]. The experiments were carried out in hexane using protic donors of substantially different pK_a values (isopropanol, pK_a = 17; benzylalcohol, pK_a = 15 and 3,4,5-trimethylphenol, pK_a = 10.6) in the temperature range from 213 to 293 K. The short time scale set by the IR pursuit was expected to allow detection of the hydrogen bonded intermediates. Contrary to this, we expected the equilibrations in the NMR experiments to be fast on the NMR timescale with concomitant signal averaging of the involved species.

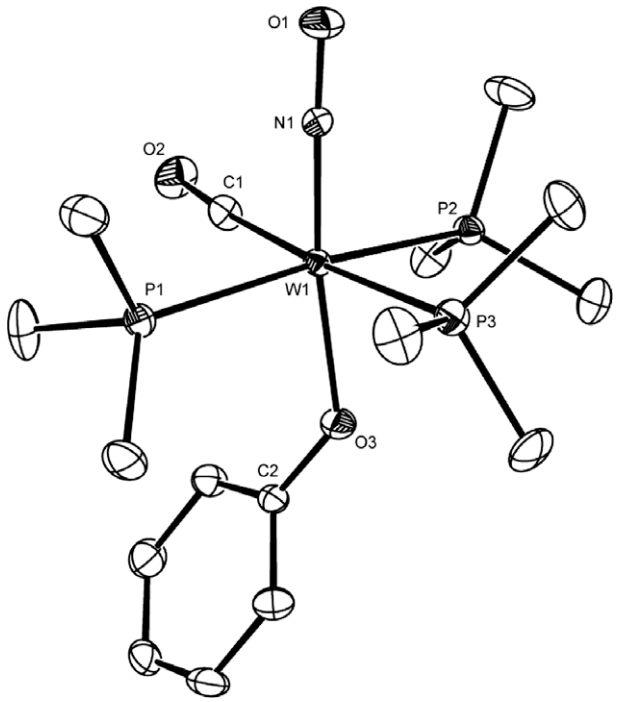

Fig. 3. View of the molecular structure of compound **2** (ellipsoids drawn at the 30% probability level). All hydrogen atoms have been omitted for clarity. Selected bond lengths (Å) and bond angles (°): W1–N1 1.800(3), W1–C1 2.009(4), W1–O3 2.102(3), W1–P1 2.5113(9), W1–P2 2.4996(9), W1–P3 2.5502(11); W1–N1–O1 177.4(3), N1–W1–O3 171.83(13), W1–O3–C2 134.8(2).

2.3. IR spectroscopic investigations

For the IR measurements in the low temperature regime, cold solutions of **1** and the protic donors were mixed at 213 K and transferred into a pre-cooled VT IR cell (d = 0.1 cm). The addition of isopropanol or benzyl alcohol to **1** in hexane caused practically no changes in the IR spectra. We concluded that hydrogen bonding of any kind appeared only to a small extent and adduct formation occurred in concentrations below the IR detection limits.

However, in the case of the mixture of **1** with 3.2 equivalents of 3,4,5-trimethylphenol (**TMP**) strong changes became visible in the IR spectrum between 1500 and 2000 cm^{-1} in the temperature range of 213–293 K (Fig. 4). A reference spectrum of **1** was practically temperature independent showing three strong bands at 1895, 1618 and 1531 cm^{-1}. In the presence of **TMP** the adducts **3a** and **3b** were formed interacting with **1** at the hydride and the O_{NO} site (K_1 and K_2 of Scheme 2). The IR spectra showed overlaid ν(CO) bands of both species falling together in a band with increased half-height width in comparison with the ν(CO) band of **1**. The band maximum of the superimposed ν(CO) bands shifted to higher wavenumbers with decreasing temperature (maximum shift of 9 cm^{-1} with respect to the corresponding band of **1** at 213 K). This relatively small ν(CO) shift suggests that the closer environment of the CO group changes only marginally upon **TMP** addition excluding that the O_{CO} atom gets involved in hydrogen bonding. Hydrogen-bonding interaction at the O_{CO} site would anyway be expected to cause a band shift in the direction opposite to what was observed [29]. Similarly when the tungsten center of **1** would get involved in hydrogen bonding with a proton donor, the ν(CO), ν(WH) and ν(NO) bands are expected to be shifted toward higher wave numbers by $\Delta\nu$ = +100–150 cm^{-1} [18–20,28,29]. No such bands were observed in the IR spectra in the presence of **TMP** concluding that such hydrogen bonding is not occurring.

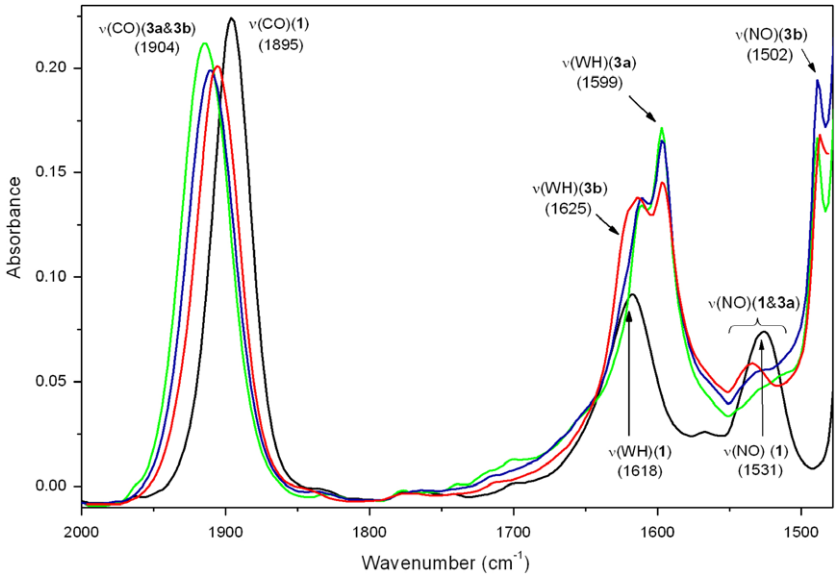

Fig. 4. IR spectrum of **1** at 213 K in hexane (black) and IR spectra of **1** in the presence of **TMP** (0.0173/0.0567 mol/L) at 213 (green), 233 (blue) and 293 K (red) in hexane. Wavenumbers of the major bands are given in brackets. (For interpretation of the references to colour in this figure legend, the reader is referred to the web version of this article.)

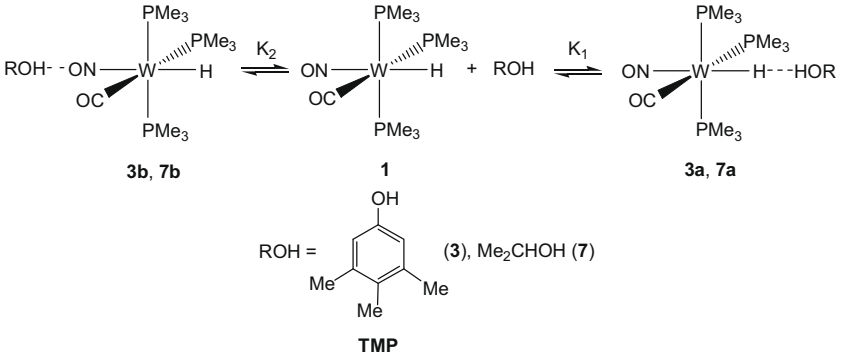

Scheme 2.

The adduct **3b** with hydrogen bonded **TMP** attached to the NO group causes indeed a new ν(NO) band at considerably lower wavenumbers appearing for all temperatures at 1502 cm^{-1} (Fig. 6). This band of **3b** is of low intensity and is located shoulder-like at the flank of a neighbouring strong band of lower wavenumbers. The strong shift of the band of **3b** with respect to ν(NO) of **1** (−29 cm^{-1}) speaks for hydrogen bonding to the O_{NO} atom [29]. The VT IR spectra of the ν(NO) region provide vague additional evidence for the dihydrogen binding equilibrium of **TMP** with **1** to form **3a**. Since hydrogen bonding to H_W can not cause much electronic perturbation at the NO ligand, the ν(NO) band of **3a** is expected to appear in relative close vicinity to the ν(NO) absorption of **1**. In the 293 K IR spectrum, for instance, a ν(NO) band appears at 1542 cm^{-1}, which is tentatively assigned to **3a**. Some ambiguity in this assignment arises from the fact that the ν(NO) bands of compounds of type **1** have generally low intensities and that species like **1**, **3a** and **3b** appear in lowered equilibrium concentrations so that the observed bands are at the detection limits.

Analyzing the ν(WH) region of the VT IR spectra, significant changes were seen upon **TMP** addition. Three overlapping bands were detected attributed to the band of free **1** at 1618 cm^{-1}, to a band for the W–H···HOR dihydrogen bonded adduct **3a** at 1599 cm^{-1} and a shoulder at around 1625 cm^{-1} attributed to **3b** with hydrogen bonding to the O_{NO} atom (Fig. 5) [29]. The intensity of the band of **3a** increases at the expense of the intensity of the ν(WH) band of **1** upon lowering of the temperature. These intensity changes are reversible indicating that the adduct formation is an equilibrium. The ν(WH) band of **3b** appearing as a shoulder to the ν(WH) of **1** persists at 293 K. Its temperature dependence was somewhat unexpected, since upon lowering of the temperature it decreases in intensity, while the ν(WH) band of **3a** gets stronger and prevails at low temperature at the expense of the corresponding band of **3b**. This can be explained in terms of a competition of the **1**/**3a** and **1**/**3b** equilibria competing for **1**. The association process to form **3a** shows the stronger temperature dependence due to a larger entropic term (vide infra). Apparently **3a** possesses a stronger dihydrogen bond and concomitant with this it achieves also a tighter solvate packing.

The **1**/**3a** and **1**/**3b** equilibria according to Scheme 2 were then quantitatively analyzed between 253 and 293 K via deconvolution of the overlapping ν(WH) bands and subsequent integration. Calculational details of the **1**/**TMP** system for the determination of the equilibrium constants K_1 of the **1**/**3a** and K_2 of the **1**/**3b** equilibria in hexane can be found in the Supplementary material.

K_1 and K_2 belonging to the two competitive processes of Scheme 2 were analyzed as a function of temperature using Eqs. (1) and (2).

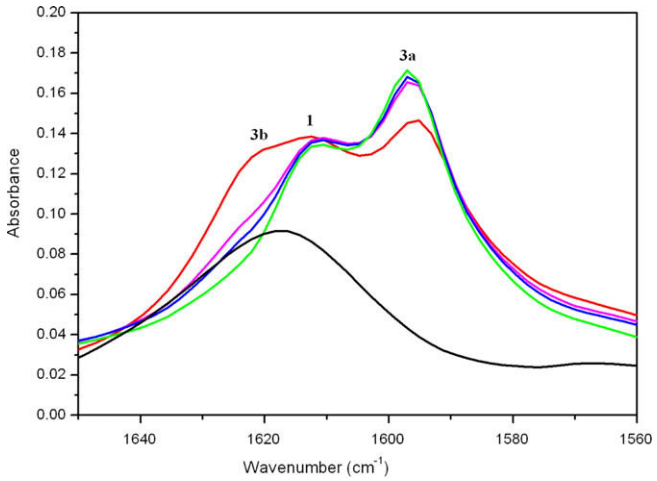

Fig. 5. Enlargement of the IR spectra in the ν(WH) region of **1** (0.0173 mol/L) at 213 K in hexane (black) and of **1** in the presence of 3.2 eq of **TMP** (0.0567 mol/L) at 213 K (green), 233 K (blue), 243 K (purple) and 293 K (red). (For interpretation of the references to colour in this figure legend, the reader is referred to the web version of this article.)

$$K_1 = [\mathbf{3a}]/[\mathbf{1}][\mathrm{ROH}] = \exp(-\Delta H_1^0/\mathrm{RT} + \Delta S_1^0/R) \quad (1)$$

$$K_2 = [\mathbf{3b}]/[\mathbf{1}][\mathrm{ROH}] = \exp(-\Delta H_2^0/\mathrm{RT} + \Delta S_2^0/R) \quad (2)$$

At all temperatures measured K_1 is larger than K_2 indicating predominance for K_1 and hydrogen bonding between H_W of **1** and **TMP** (dihydrogen bonding) (Fig. 6). At 253 K for instance, K_1 is approx. 3 times larger than K_2. The temperature dependencies of $\ln(K_1)$ and $\ln(K_2)$ vs. $1/T$ according to Eqs. (1) and (2) allowed to extract enthalpies: $\Delta H_1 = -5.8 \pm 0.4$ and $\Delta H_2 = -2.8 \pm 0.1$ kcal/mol and entropies: $\Delta S_1 = -15.3 \pm 1.4$ and $\Delta S_2 = -5.8 \pm 0.3$ e.u. The $-\Delta S$ values lie in the typical range of 5–20 e.u. reported for hydrogen bonding in organic systems [2,12,29,81,82] and additionally stress that dihydrogen bonding in **3a** is prevalent over hydrogen bonding in **3b** and has the higher temperature gradient.

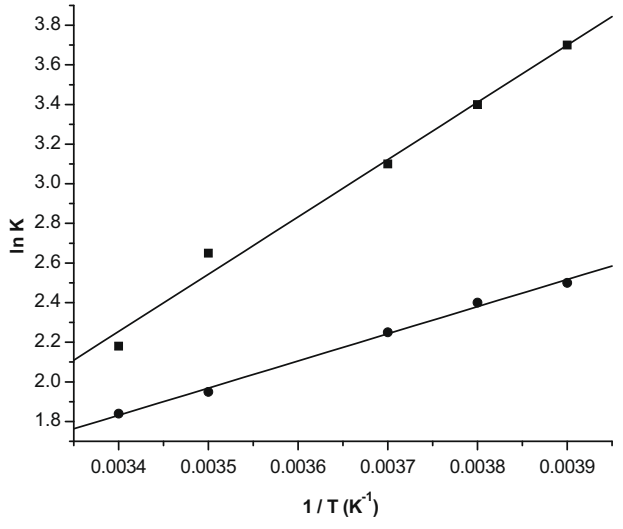

Fig. 6. van't Hoff plots of the two hydrogen bonding equilibria K_1 and K_2 of **1** (0.0173 mol/L) and **TMP** (0.0567 mol/L) in hexane forming the adducts **3a** (●) and **3b** (■) according to K_1 and K_2 of Scheme 2. The equilibrium constants were calculated from the concentrations of the equilibrium species derived from the deconvoluted ν(WH) bands of Fig. 5.

2.4. ^{1}H NMR spectroscopic investigations

^{1}H NMR spectroscopy is well-suited for probing hydrogen bonding through hydride ligands using titrations as quantitative experiments [9–11,23,27,29]. The equilibration processes of Scheme 2 were expected to be fast on the NMR time scale with concomitant signal averaging. We studied the cases of the interaction of **1** with isopropanol and **TMP** as weak and strong protic donor binding cases.

First we pursued changes in the chemical shifts by ^{1}H NMR spectroscopy occurring upon addition of the protic donors to **1**. Solutions of **1** were pre-mixed with various ratios of isopropanol and **TMP** at temperatures below −55 °C and then the chemical shifts of the hydride resonance were determined at various temperatures. The plots of the chemical shift differences ($\Delta\delta$) vs. $T(K)$ are presented in the Supplementary material (Figs. S2 and S3). The averaged signals of the hydrogen bonded adducts **7a,b** with isopropanol in toluene-d_8 showed upfield shifted $\Delta\delta$ values, which became more pronounced when the concentration of isopropanol was increased or the temperature lowered. The $\Delta\delta$ values of **3a,b** displayed higher values of $\Delta\delta$ in comparison with **7a,b** apparently due to a stronger interaction with the hydride ligand.

T_1 ^{1}H NMR experiments of **1** with isopropanol and **TMP** exhibited substantially shorter T_1 of the H_W nucleus, once the acidic substrate was added (see Figs. S4 and S5 in Supplementary material), with higher concentrations of the alcohols, the minima of the pseudo-parabolae shift toward higher temperatures and shorter relaxation times. The T_1 values were significantly shorter for the addition of **TMP**. This reflects a larger equilibrium shift according to Scheme 2 toward the dihydrogen bonded adducts with **TMP** than with isopropanol. These T_1 results obtained in the presence of different concentrations of the alcohols are fully consistent with the conclusions reached from the chemical shift experiments.

VT NMR spectroscopy can also provide thermodynamic data and geometrical parameters of dihydrogen bonding [27,29] attained via titrations, in our case with changes of the concentrations of the added protic donors. Changes in the equilibrium positions of Scheme 2 would be expressed as chemical shift changes ($\Delta\delta$ method), while in the case of the ^{1}H T_1 NMR measurements changes in the equilibrium positions would be expected to cause changes in the excess relaxation rates ($\Delta R_1(\mathrm{min}) = 1/T_1(\mathrm{min})(\mathrm{add}) - 1/T_1(\mathrm{min})(\mathrm{WH})$) ($\Delta R_1(\mathrm{min})$). Equilibrium constants $K_{(\Delta\delta)}$ and $K_{(\Delta R_1)}$ were obtained via pursuit of the changes in the chemical shifts of the H_W signal ($\Delta\delta$) or of the excess relaxation rates ($\Delta R_1(\mathrm{min})$) and via curve fitting of the plots of these parameters of H_W vs. concentrations of the protic donors. All hydride components of the equilibria of Scheme 2 average to one H_W signal. The $\Delta\delta$ method is expected to show response for both equilibria of Scheme 2, while the $\Delta R_1(\mathrm{min})$ method was expected to be sensitive merely to changes of the closer chemical environment of the hydride ligand of **1**, thus specifically addressing interactions with H_W of **3a** and **7a** only, while the equilibrium interactions with O_{NO} of **7b** and **3b** are expected to stay with this method "silent". The strength of hydrogen bonding is solvent dependent and in more polar solvents the equilibria are expected to shift toward the dissociated side. Since relatively small equilibrium constants were expected to evolve, we used the least polar solvent applicable, which was toluene with practical solubilities for all reaction components at all temperatures.

The $K_{(\Delta\delta)}$ and $K_{(\Delta R_1)}$ values obtained for the hydrogen bonded adducts of isopropanol with **1** showed similar dependencies in temperature and the van't Hoff plots of lnK vs. 1/T (Eq. (1), (2)) produced satisfactory linear regressions (Fig. 7). The thermodynamic data calculated from $K_{(\Delta\delta)}$ and $K_{(\Delta R_1)}$ values were similar ($\Delta H_{(\Delta\delta)} = -2.3$ kcal/mol; $\Delta S_{(\Delta\delta)} = -11.7$ e.u. and $\Delta H_{(\Delta R_1)} = -2.9$ kcal/mol; $\Delta S_{(\Delta R_1)} = -14.6$ e.u.) presumably indicating that involvement of

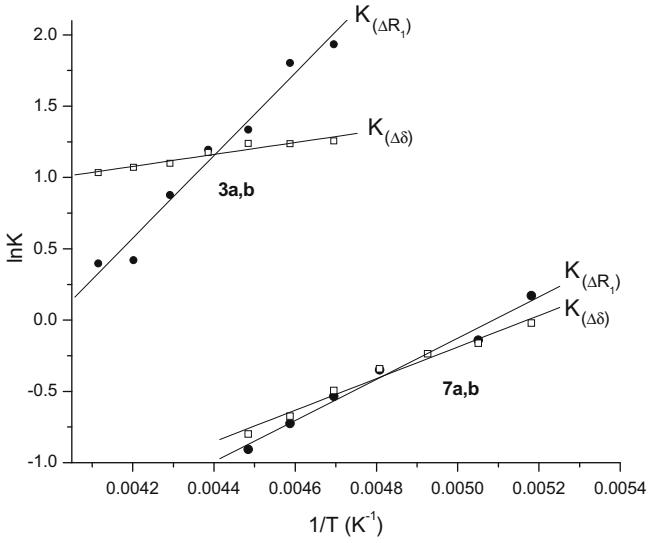

Fig. 7. van't Hoff plots ln$K$ vs. $1/T$ for the adduct equilibria of **1** with **TMP** or isopropanol forming **3a,b** or **7a,b** in d_8-toluene. The K values were derived from NMR titrations observing the chemical shifts of HW, ($\Delta\delta$) or the changes in the excess relaxation rates of HW ($\Delta R1$) in dependence of the concentration of the protic donors.

the hydrogen bonding equilibrium with O_{NO} leading to **7b** is very small and practically non-existent.

In the case of the adduct formation of **1** with **TMP** producing **3a** and **3b**, the van't Hoffs plots showed also good linear regressions, however, with quite different slopes for $K_{(\Delta\delta)}$ and $K_{(\Delta R_1)}$ (Fig. 7) and consequently with large differences in the calculated thermodynamic data ($\Delta H_{(\Delta\delta)} = -0.8$ kcal/mol; $\Delta S_{(\Delta\delta)} = -1.4$ e.u. and $\Delta H_{(\Delta R_1)} = -5.8$ kcal/mol; $\Delta S_{(\Delta R_1)} = -22.9$ e.u.). This is interpreted in terms of the appearance of stronger hydrogen bonding to O_{NO} implicitly contained in the $\Delta\delta$ measurements, but not in the ΔR_1 measurements. The hydrogen bonding equilibrium of the proton of **TMP** with the O_{NO} group of **3b** (also evidenced from the IR spectroscopic studies) interferes strongly in the averaging of the chemical shifts of H_W and the calculated $K_{(\Delta\delta)}$ values are indeed a mixture of both the K_1 and K_2 values according to Scheme 2. The $K_{(\Delta R_1)}$ values represent only dihydrogen bonding interaction with the hydride ligand of **1** to form **3a**.

As described in the previous chapter the ΔH of the interaction of **1** with **TMP** was also determined by IR spectroscopy in the temperature range of 253–293 K (Table 1). Equilibrium constants were directly calculated from the scaled band intensities. The only difference between the IR and the NMR experiments was the solvent used: hexane vs. toluene, as unpolar solvents these apparently did not cause great differences. Thus, the ΔH values obtained for the formation of **3a** by both the IR and the ΔR_1 method agree very well showing exactly the same value of -5.8 kcal/mol (Table 1). The ΔH for the interaction in **3b** could reliably be obtained only by the IR method (2.8 kcal/mol). The studies of hydrogen-bonding interactions of rhenium hydrides reported earlier with fluorinated alcohols in hexane and in toluene showed similar qualitative agreement [27].

The small negative free energy difference ΔG of ca. -0.9 kcal/mol of the IR derived results for **1** and **TMP** was in favour of K_1 with **3a** over K_2 with **3b**. The $K_{(\Delta R_1)}$ values of **7a** were determined to be less than 1 L/mol in the temperature range of 193–223 K, which goes along with the very small positive free energy differences revealing that the formation of any hydrogen bonded adduct of **1** with the weak acid isopropanol is generally less favourable. The twice higher negative value of $\Delta H_{(\Delta R_1)}$ of **3a** than of **7a** (Table 1) confirmed much stronger hydrogen-bonding interaction between **1** and the more acidic **TMP**. It was also worth analyzing the entropy effects of the hydrogen bonding adducts, although these are expected to possess greater errors. The ΔS value of **3a** observed by IR spectroscopy has a slightly smaller negative value than ΔS obtained by the T_1 NMR spectroscopic measurements (ΔR_1) (Table 1). A lower ΔS value was determined by the IR analyses in hexane, which might be explained by a solvent effect and a somewhat different self-association process of the free **TMP** in hexane and toluene solution.

The dihydrogen bond distance r(H···H) [Å] obtained from $r(H\cdots H) = 5.817(\nu\cdot\Delta R_1(\min))^{-1/6}$ are 2.1 Å for the dihydrogen bonding between **1** and isopropanol (**7a**) and 1.9 Å for the one between **1** and **TMP** (**3a**) (Table 1) showing a difference in the contact distance of 0.2 Å. The 1.9 Å intermolecular bonding of **3a** expresses a relatively strong interaction, while the 2.1 Å contact of **7a** is weak, falling into the upper range for dihydrogen bonding interactions (1.7–2.2 Å) [1,2,29].

Table 1
IR and NMR derived ΔH and ΔS values and H···H distance in hexane (IR) or d_8-toluene (NMR) for the hydrogen bonding adducts **3a,b** and **7a,b** with reference to Figs. 6 and 7.

Equilibrium and method	ΔH (kcal/mol)	ΔS (e.u.)	r(H···H) (Å)
$K_{(\Delta R_1)}$ (**7a**)	-2.9 ± 0.2	-14.6 ± 1.0	2.1
$K_{(IR)}$ (**3a**)	-5.8 ± 0.1	-15.3 ± 0.3	
$K_{(IR)}$ (**3b**)	-2.8 ± 0.1	-5.8 ± 0.3	
$K_{(\Delta R_1)}$ (**3a**)	-5.8 ± 0.4	-22.9 ± 1.9	1.9

3. Conclusion

Protonation of **1** with various ROH protic donors produced organyloxide complexes with evolution of H_2. Experimental evidence was provided for intermolecular dihydrogen bonding between **1** and the protic donors, which might precede the H_2 evolution process. In general hydrogen-bonding interactions are equilibria and therefore dependent on temperature and type of solvent, the ROH concentration, the ROH acid strength and to some extent also on steric effects. IR experiments at low temperatures revealed in the case of the protic donor **TMP** the expected dihydrogen bonding to H_W of **1** (**3a**) and another competitive equilibrium process of hydrogen bonding to the O_{NO} group to form **3b**. The interaction enthalpies of **3a** observed in the IR (ΔH_1) and NMR titrations ($\Delta H_{(\Delta R_1)}$) gave the same value of -5.8 kcal/mol demonstrating excellent agreement between these different spectroscopic methodologies. From NMR relaxation time measurements of the hydride ligand of **1** in d_8-toluene, a shorter dihydrogen bonding distance value was derived for **3a** than for **7a** demonstrating the pK_a dependence of the dihydrogen bonding interactions and stressing the involvement of such species as intermediates in the protonation of hydridic transition metal hydrides.

4. Experimental

4.1. General considerations

All reactions and manipulations were performed under an atmosphere of dry nitrogen using conventional Schlenk techniques or a glove box. Solvents were dried by standard methods and freshly distilled before use. Reagents of commercial quality were obtained from commercial suppliers and used as received. NMR spectra were recorded on the following spectrometers: Varian Gemini-200 instrument; ^{1}H at 199.98 MHz, ^{13}C at 50.29 MHz, ^{19}F

at 188.15 MHz, ^{31}P at 80.95 MHz. Varian Gemini-300 instrument; ^{1}H at 300.08 MHz, ^{13}C at 75.46 MHz, ^{19}F at 282.33 MHz, ^{31}P at 121.47 MHz. Bruker DRX-500 instrument; ^{1}H at 500.13 MHz, ^{13}C at 125.23 MHz, ^{31}P at 202.51 MHz. Chemical shifts δ (^{1}H) and δ (^{13}C) were recorded rel. to the solvent, δ (^{19}F) rel. to $CFCl_3$, and δ (^{31}P) rel. to H_3PO_4. All NMR spectra were recorded at room temperature unless otherwise stated. The two *trans* phosphines are referred to as "PMe_3 *trans*". IR spectra: Biorad FTS-45 and FTS-3500 instruments. Mass spectra: Finnigan-MAT-8400 spectrometer; FAB spectra in 3-nitrobenzyl alcohol matrix. Elemental analyses: Leco CHN(S)–932 instrument. *mer*-W(CO)(H)(NO)(PMe_3)$_3$ **1** was prepared according to a published procedure [64].

4.2. Preparation of mer-W(CO)(NO)(OC_6H_5)(PMe_3)$_3$ (**2**)

Orange **2** was prepared via the reaction of **1** (13 mg, 0.028 mmol) with phenol (2.7 mg, 0.028 mmol) in toluene-d_8 (0.7 mL) at 60 °C stirring for 4 h. Yield: 11 mg (70%). IR (cm^{-1}, pentane): 1910 (CO), 1584 (NO). ^{1}H NMR (300.0 MHz, C_6D_6): δ 7.24 (m, 2H, Ph), 6.67 (m, 3H, Ph), 1.22 (m, 18H, 2 PMe_3 *trans*), 1.11 (d, $^{2}J_{HP}$ = 7 Hz, 9H, 1 PMe_3). ^{13}C{^{1}H} NMR (125.2 MHz, C_6D_6): δ 228.3 (dt, $^{2}J_{CP(trans\ to\ CO)}$ = 55 Hz, CO), 168.2 (m, Ph), 129.6 (s, Ph), 119.5 (s, Ph), 115.2 (m, Ph), 18.3 (m, 2 PMe_3 *trans*), 17.1 (dt, $^{1}J_{CP}$ = 21 Hz, $^{3}J_{CP}$ = 3 Hz, 1 PMe_3). ^{31}P{^{1}H} NMR (121.5 MHz, C_6D_6): δ −23.0 (d with satellites, $^{2}J_{PP}$ = 19 Hz, $^{1}J_{PW}$ = 289 Hz, 2 PMe_3 *trans*), −26.9 (t with satellites, $^{2}J_{PP}$ = 19 Hz, $^{1}J_{PW}$ = 239 Hz, 1 PMe_3). FAB-MS: *m/z* 563 [M$^+$], 535 [M$^+$–CO], 487 [M$^+$–PMe_3]. Anal. Calc. for $C_{16}H_{32}NO_3P_3W$: C, 34.12; H, 5.73; N, 2.49. Found: C, 34.51; H, 5.48; N, 2.34%.

4.3. Preparation of mer-W(CO)(NO)(O(3,4,5-$Me_3C_6H_2$))(PMe_3)$_3$ (**3**)

To a solid mixture of 1 eq of **1** (0.030 g, 0.064 mmol) and 1.1 eq of 3,4,5-trimethylphenol (0.0095 g, 0.070 mmol) was added 1 ml of toluene-d_8. After 5 h at 60 °C the reaction was complete (NMR monitoring). The solvent was removed in vacuum and the residue was recrystallized from THF at −30 °C to give an orange–yellow solid of **3**. Yield: 0.033 g (85%). IR (cm^{-1}, pentane): 1582 (NO); 1908 (CO). **^{1}H** NMR (200 MHz, THF-d_8, 25 °C): δ 1.30 (m, 18H, 2PMe_3, trans), 1.10 (d, 9H, 1PMe_3), 6.70 (s, 2H, Ph), 2.01 (s, 6H, 2CH_3 from Ph), 1.91 (s, 3H, CH_3 from Ph). ^{31}P{^{1}H} NMR (80.9 MHz, THF-d_8, 25 °C): δ −30.3 (t with satellites $^{2}J_{PP}$ = 19.9 Hz, $^{1}J_{PW}$ = 300 Hz, 1 PMe_3), −26.0 (d with satellites, $^{2}J_{PP}$ = 19.9 Hz, $^{1}J_{PW}$ = 350 Hz, 2 PMe_3, *trans*). ^{13}C{^{1}H} NMR (50.3 MHz, THF-d_8, 25 °C): δ 228.6 (dt, $^{2}J_{CP(trans\ to\ CO)}$ = 56 Hz, $^{2}J_{CP(cis\ to\ CO)}$ = 6 Hz, CO), 166.5 (s, Ph), 135.2 (s, Ph), 119.7 (s, Ph), 118.0 (s, Ph), 21.0 (s, CH_3 from Ph), 14.2 (s, CH_3 from Ph), 18.6 (td, $^{1}J_{CP}$ = 12.3 Hz, $^{3}J_{CP}$ = 2.1 Hz, 2 PMe_3, *trans*), 17.6 (dt, $^{1}J_{CP}$ = 20.0 Hz, $^{3}J_{CP}$ = 3 Hz, PMe_3). Anal. Calc. for $C_{19}H_{38}NO_3P_3W$: C, 37.69; H, 6.28; N, 2.31. Found: C, 37.90; H, 6.23; N, 2.38%.

4.4. Preparation of mer-W(CO)(NO)(OCH_2CF_3)(PMe_3)$_3$ (**4**)

Yellow–orange **4** was prepared using the same procedure as for **3**, reacting **1** (20 mg, 0.042 mmol) and 2,2,2-trifluoroethanol (9.3 μL, 0.127 mmol) in toluene-d_8 (0.8 mL) at 60 °C for 1 d. Yield: 15 mg (62%). IR (cm^{-1}, pentane): 1908 (CO), 1580 (NO). ^{1}H NMR (300.0 MHz, C_6D_6): δ 3.86 (q, $^{3}J_{HF}$ = 10 Hz, 2H, –OCH_2–), 1.26 (m, 18H, 2 PMe_3 *trans*), 1.03 (d, $^{2}J_{HP}$ = 6 Hz, 9H, 1 PMe_3). ^{13}C{^{1}H} NMR (125.2 MHz, C_6D_6): δ 229.0 (m, CO), 128.1 (q, $^{1}J_{CF}$ = 282 Hz, -CF_3), 71.8 (dtq, $^{2}J_{CF}$ = 31 Hz, $^{3}J_{CP(trans\ to\ CO)}$ = 8 Hz, $^{3}J_{CP(cis\ to\ CO)}$ = 2 Hz, –OCH_2–), 18.2 (m, 2 PMe_3 *trans*), 16.8 (m, 1 PMe_3). ^{19}F NMR (282.3 MHz, C_6D_6): δ -78.7 (t, $^{3}J_{FH}$ = 10 Hz, –CF_3). ^{31}P{^{1}H} NMR (202.5 MHz, C_6D_6): δ −24.6 (m, 2 PMe_3 *trans*), -25.4 (m, 1 PMe_3). EI-MS: *m/z* 569 [M$^+$], 541 [M$^+$–CO], 465 [M$^+$–CO–PMe_3]. Anal. Calc. for $C_{12}H_{29}F_3NO_3P_3W$: C, 25.32; H, 5.14; N, 2.46. Found: C, 25.40; H, 5.04; N, 2.44%.

4.5. Preparation of mer-W(CO)(NO)(OCH_2Ph)(PMe_3)$_3$ (**5**)

Compound **1** (21 mg, 0.044 mmol) was dissolved in C_6D_6 (0.7 mL), and benzyl alcohol (5 μL, 0.066 mmol) was added. After 1 d NMR monitoring at 60 °C the reaction was complete and the solvent removed *in vacuo*. The residue was extracted with pentane (0.5 mL), the solution filtered, and orange **5** crystallized at −30 °C. Yield: 20 mg (78%). IR (cm^{-1}, pentane): 1904 (CO), 1572 (NO). ^{1}H NMR (300.0 MHz, C_6D_6): δ 7.36 (m, 2H, Ph), 7.26 (m, 2H, Ph), 7.10 (m, 1H, Ph), 4.86 (s, 2H, –OCH_2–), 1.29 (m, 18H, 2 PMe_3 *trans*), 1.13 (d, $^{2}J_{HP}$ = 7 Hz, 9H, 1 PMe_3).^{13}C{^{1}H} NMR (125.2 MHz, C_6D_6): δ 229.2 (dt, $^{2}J_{CP(cis\ zu\ CO)}$ = 6 Hz, $^{2}J_{CP(trans\ zu\ CO)}$ = 54 Hz, CO), 149.4 (s, Ph), 127.7 (s, Ph), 125.7 (s, Ph), 125.5 (s, Ph), 75.8 (dt, $^{3}J_{CP(cis\ zu\ CO)}$ = 1 Hz, $^{3}J_{CP(trans\ zu\ CO)}$ = 8 Hz, –OCH_2–), 18.2 (m, 2 PMe_3 *trans*), 17.2 (dt, $^{1}J_{CP}$ = 20 Hz, $^{3}J_{CP}$ = 3 Hz, 1 PMe_3). ^{31}P{^{1}H} NMR (121.5 MHz, C_6D_6): δ −25.2 (m mit Satelliten, 2 PMe_3 *trans*), −26.2 (m mit Satelliten, 1 PMe_3). MS (EI, 70 eV): *m/z* 577 [M$^+$], 549 [M$^+$–CO], 501 [M$^+$–PMe_3], 473 [M$^+$–CO–PMe_3], 321 [M$^+$–CO–3 PMe_3], 291 [M$^+$–CO–3 PMe_3–NO]. Anal. Calc. for $C_{17}H_{34}NO_3P_3W$: C, 35.37; H, 5.94; N, 2.43. Found: C, 35.12; H, 5.54; N, 2.35%.

4.6. Preparation of mer-W(CO)(NO)(OCH_3)(PMe_3)$_3$ (**6**)

mer-W(CO)(H)(NO)(PMe_3)$_3$ **1** (16 mg, 0.034 mmol), was dissolved in C_6D_6 (0.7 mL), and methanol (4 μL, 0.099 mmol) was added. After 1 d at 60 °C the solvent was removed *in vacuo*. The residue was extracted with pentane (0.5 mL), the solution filtered, and orange **6** crystallized at −30 °C. Yield: 14 mg (82%). IR (cm^{-1}, pentane): 1904 (CO), 1569 (NO). ^{1}H NMR (300.0 MHz, C_6D_6): δ 3.92 (m, 3H, -OCH_3), 1.36 (m, 18H, 2 PMe_3 *trans*), 1.11 (d, $^{2}J_{HP}$ 7 Hz, 9H, 1 PMe_3). ^{13}C{^{1}H} NMR (125.2 MHz, C_6D_6): δ 229.2 (dt, $^{2}J_{CP(trans\ to\ CO)}$ = 55 Hz, $^{2}J_{CP(cis\ to\ CO)}$ = 6 Hz, CO), 62.2 (dt, $^{3}J_{CP(trans\ to\ CO)}$ = 9 Hz, $^{3}J_{CP(cis\ to\ CO)}$ = 1 Hz, –OCH_3), 18.2 (m, 2 PMe_3 *trans*), 17.1 (dt, $^{1}J_{CP}$ = 20 Hz, $^{3}J_{CP}$ = 3 Hz, 1 PMe_3). ^{31}P{^{1}H} NMR (121.5 MHz, C_6D_6): δ −24.4 (m with satellites, 2 PMe_3 *trans*), -26.7 (m with satellites, 1 PMe_3). EI-MS: *m/z* 501 [M$^+$], 473 [M$^+$–CO], 397 [M$^+$–CO–PMe_3]. For this compound no satisfactory elemental analysis could be obtained.

4.7. Preparation of mer-W(CO)(NO)[$OCHMe_2$](PMe_3)$_3$ (**7**)

Compound **1** (28 mg, 0.058 mmol), was dissolved in C_6D_6 (0.7 mL), and isopropanol (18 μL, 0.232 mmol) was added. After 3 d at 60 °C the solvent was removed *in vacuo*. The residue was extracted with pentane (0.5 mL), the solution filtered, and yellow–orange **7** crystallized at −30 °C. Yield: 21 mg (68%). IR (cm-1, pentane): 1905 (CO), 1565 (NO). ^{1}H NMR (300.0 MHz, C_6D_6): δ 3.73 (sept, $^{3}J_{HH}$ = 6 Hz, 1H, –OC*H*Me_2), 1.37 (m, 18H, 2 PMe_3 *trans*), 1.09 (d, $^{2}J_{HP}$ = 6 Hz, 9H, 1 PMe_3), 1.05 (d, $^{3}J_{HH}$ = 6 Hz, 6H, –CH_3). ^{13}C{^{1}H} NMR (125.2 MHz, C_6D_6): δ 229.4 (m, CO), 70.9 (m, –O*C*HMe_2), 28.8 (s, –CH_3), 18.3 (m, 2 PMe_3 *trans*), 16.8 (m, 1 PMe_3). ^{31}P{^{1}H} NMR (121.5 MHz, C_6D_6): δ –27.9 (m mit Satelliten, 3 PMe_3). (EI-MS): *m/z* 529 [M$^+$], 501 [M$^+$–CO], 425 [M$^+$–O–PMe_3], 349 [M$^+$–CO–2 PMe_3]. Anal. Calc. for $C_{13}H_{34}NO_3P_3W$: C, 29.51; H, 6.48; N, 2.65. Found: C, 29.45; H, 6.05; N, 2.68%.

4.8. Quantitative NMR pursuits of the reaction of **1** with protic donors

Kinetic measurements were carried out on a Varian-Gemini-200 spectrometer (80.9 MHz, ^{31}P{^{1}H}). 20 mg of **1** (0.0425 mmol) was dissolved in 0.7 ml of toluene-d_8 and 8.0 mg of phenol (0.085 mol/L); 11.6 mg of 3,4,5-trimethylphenol (0.085 mol/L); 9.3 μL of trifluoroethanol (0.1275 mmol); 13.2 μL of benzylalcohol

(0.1275 mmol); 5.2 μL of methanol (0.1275 mmol) and 9.8 μL of isopropanol (0.1275 mmol) were placed in a Young tap NMR tube. The rate of formation of the alkoxide complexes **2**–**7** and H_2 evolution were monitored by integration of the phosphine doublets and the triplet resonances of hydride **1** at –29.8 and –35.1 ppm in the $^{31}P\{^1H\}$ NMR spectra at every 8.5 min (**2**), 9.3 min (**3**), 32.5 min (**4**), 32.5 min (**5**), 32.5 min (**6**) and 97.6 min (**7**) at 60 °C. The reactions of formation of **2**–**7** were over after 4 h (**2**), 5 h (**3**), 20 h (**4**), 24 h (**5**), 24 h (**6**) and 72 h (**7**) when **1** was completely consumed. Plot of the decay of [**1**] vs. time *t* allowed exponentional fitting with a first order law. From the slope of the linear plot of lnc vs. time *t*, the rate constant *k* was determined. The half-life times of the reactions $t_{1/2}$ were calculated based on the expression $t_{1/2} = \ln 2/k$ [83].

4.9. Quantitative IR analysis of hydrogen bonding of 1 with 3,4,5-trimethylphenol in the ν(WH) region

For these studies, the Merlin Software [84] was used to carry out quantitative analysis using the Lambert–Beer law. The Lambert–Beer law is defined by the linear relationship between the absorption and the concentration of the sample:

$$A_\lambda = \varepsilon_\lambda \cdot b \cdot c$$

where A_λ is the absorbance value of the sample at specific wavelength, in our case at 1618 cm^{-1} (ν(W–H) band), ε_λ is the molar absorptivity at the wavelength (L mol^{-1} cm^{-1}), b is path length through the sample (b = 0.1 cm) and c is the concentration of the sample (mol/L). The calibration was carried out with linear curves of known concentrations of **1** in hexane (c = 0.0030, 0.0064, 0.0110, 0.0191, 0.0232, 0.0364 and 0.0490 mol/L) in dependence of the measured peak areas (or absorbances) of the selected ν(W–H) band at 1618 cm^{-1} in the temperature range of 253–293 K. Furthermore, quantitative IR experiments were carried out involving a mixture of 4.1 mg of **1** (0.0173 mol/L) and 3.9 mg (0.0567 mol/L) of 3,4,5-trimethylphenol in 0.5 ml of hexane. The temperature was varied and the spectra were measured every 10 K starting from 253 K to 293 K. In the IR spectra the three overlapping bands of the dihydrogen bonded species $C_6H_2(CH_3)_3OH\cdots H–W(CO)(N-O)(PMe_3)_3$ (**3a**) at 1599 cm^{-1}, of the free hydride **1** at 1618 cm^{-1} and of the dihydrogen bonding species $C_6H_2(CH_3)_3OH\cdots ON–W(CO)(H)(PMe_3)_3$ (**3b**) at 1625 cm^{-1} were deconvoluted using a programme with a Lorentzian line function [85] and then the equilibrium concentrations of the species [**3a**], [**1**] and [**3b**] were determined using the calibration curves of **1** at each temperature. In these calculations we used for the two adducts **3a** and **3b** the same extinction coefficients for the W–H bands and we have good indication that the error stays within acceptable limits. The initial concentration of **1** should be the sum of concentrations of all the species **1**, **3a** and **3b** in equilibrium. Based on the peak areas calibrated to hydride **1**, the overall deviations of the sum of concentrations from 100% are in the range of 3.9–8.7%. The equilibrium concentrations of 3,4,5-trimethylphenol were calculated from the initial concentration of $C_6H_2(CH_3)_3OH$ by the relation: $[C_6H_2(CH_3)_3OH] = [C_6H_2(CH_3)_3OH]_{initial} - [\mathbf{3a}]-[\mathbf{3b}]$. The equilibrium constants K_1 and K_2 were calculated by the equations:

$$K_1 = [\mathbf{3a}]/[\mathbf{1}][C_6H_2(CH_3)_3OH] \quad (1)$$

$$K_2 = [\mathbf{3b}]/[\mathbf{1}][C_6H_2(CH_3)_3OH] \quad (2)$$

The calculated equilibrium constants K_1 and K_2 were fitted by van't Hoff linear regressions. From the van't Hoff linear plots of $\ln K_1$ and $\ln K_2$ vs. $1/T$, the enthalpies ΔH_1 and ΔH_2 with errors of 7% and 4% and the entropies ΔS_1 and ΔS_2 with errors of 9% and 5% were determined.

4.10. Qualitative analysis of hydrogen bonding of 1 with isopropanol and 3,4,5-trimethylphenol using VT ^{1}H NMR spectroscopy

^{1}H and T_1 NMR experiments were obtained on a Bruker DRX-500 spectrometer (500 MHz, ^{1}H). The inversion-recovery method (180-τ-90) was used to determine T_1 relaxation times. The calculation of the relaxation times was made using the nonlinear three-parameter fitting routine of the spectrometer. In each experiment, the waiting period was 10 times the expected relaxation time and 12 variable delays were employed. The duration of the pulses was controlled at every studied temperature. Dihydrogen bonding is solvent dependent and for this reason toluene-d_8 was used as one of the least polar solvents which still provided good solubility of all reaction components especially at low temperature.

4.11. Equilibrium analysis of the dihydrogen bonded adducts 7a (WH···HOCHMe$_2$) and 7b (W–NO···HOCHMe$_2$) obtained from 1 and isopropanol

A solution of **1** (20 mg of **1** in 0.7 ml of toluene-d_8, c_t(WH) = 0.061 mol/L) was prepared in an NMR tube below 223 K and the chemical shifts δ(WH) and the temperature-dependent minimum relaxation time T_1(min)(WH) of the hydride ligand of **1** were determined in the temperature range of 193–228 K. Then, five different solutions of 20 mg of **1** in 0.7 ml of toluene-d_8 (c_t(WH) = 0.061 mol/L) with various concentrations of isopropanol (c(alc) = 0.0671, 0.1080, 0.1921, 0.2446 and 0.3019 mol/L) at temperature below 223 K were prepared in the NMR tubes sealed with the Teflon caps. The chemical shifts δ(eq) and the values T_1(min)(eq) of the hydride ligand of **1** were determined at every 5 K from 193 to 228 K. VT NMR titrations were used in order to extract and compare equilibrium constants $K_{(\Delta\delta)}$ and $K_{(\Delta R_1)}$ from the given changes in the chemical shift differences ($\Delta\delta = \delta$(eq) - δ(WH)) and from the given changes in the excess relaxation rates (ΔR_1(min) = $1/T_1$(min)(eq)–$1/T_1$(min)(WH)) by curve fitting.

The equilibrium constants $K_{(\Delta\delta)}$ and $K_{(\Delta R_1)}$ were calculated from Eqs. (3)–(6).

$$K = c(\text{add})/c(\text{WH}) \cdot c(\text{alc}) \quad (3)$$

$$\delta(\text{eq}) = \delta(\text{WH}) + (\delta(\text{add}) - \delta(\text{WH})) \cdot X(\text{add}) \quad (4)$$

$$1/T_1(\text{min})(\text{eq}) = 1/T_1(\text{min})(\text{add}) \cdot X(\text{add}) + 1/T_1(\text{WH}) \cdot X(\text{WH}) \quad (5)$$

$$1/T_1(\text{min})(\text{add}) = (1/T_1(\text{min})(\text{eq}) - 1/T_1(\text{WH}) \cdot X(\text{WH}))/X(\text{add}) \quad (6)$$

c(add), c(WH) and c(alc) ofEq. (3) are the equilibrium concentrations of **7a,b** or **3a,b**, **1** and the protic donors, respectively, and K is the equilibrium constant. $\delta(eq)$ of Eq. (4) is the averaged equilibrium chemical shift of δ(WH) and δ(add), δ(WH) and δ(add) are the chemical shifts of **1** and **7a,b** or **3a,b**, respectively. $c_t(WH)$ and c_t(alc) are the initial concentrations of **1** and of the alcohols. X(add) = $(0.5/c_t(\text{WH}))\cdot c_t(\text{WH}) + c_t(\text{alc}) + 1/K - (c_t(\text{WH}) + c_t(\text{alc}) + 1/K)^2 - 4c_t(\text{WH})\cdot c_t(\text{alc})^{1/2}$ is the molar fraction of **7a,b** or **3a,b**, which is obtained from the curve fitting of the experimental data of Eq. (3). T_1(min)(eq) ofEq. (5) is the equilibrium-averaged temperature-dependent minimum relaxation time; T_1(WH) is the relaxation time of **1** at the temperature of T_1(min); T_1(min)(add) and T_1(min)(WH) are the temperature–dependent minimum relaxation times of the hydride ligands of **7a** or **3a** and **1**, respectively. X(WH) and X(add) are the molar fractions of complexes **1** and **7a** or **3a** at the temperature of T_1(min)(eq).

Eqs. (4) and (5) represent the basic equations of the NMR titration experiments [12,27,86], which can be approached by curve fit-

ting of the curves of $\delta(eq)$ and $1/T_1(\min)(eq)$ vs. the initial alcohol concentrations c_t(alc). The K values were obtained by nonlinear fits using a Levenberg–Marquardt algorithm.[45] For this purpose, Eq. (7) (modified Eq. (4)) [87] was used (see below) where $Q = 0.5 \cdot (S-a)$, $S = (a^2 + 4 \cdot K \cdot c_t(\mathrm{WH}))^{1/2}$ and $a = K \cdot (c_t(\mathrm{WH}) - c_t(\mathrm{alc})) + 1$.

$$\delta(\mathrm{eq}) = (\delta(\mathrm{WH}) + Q \cdot \delta(\mathrm{add}))/(1+Q) \quad (7)$$

In this way, the association constants $K_{(\Delta\delta)}$ and $K_{(\Delta R_1)}$ for the adduct formation reaction were determined at different temperatures and then X(add) and X(WH) were calculated by solving Eq. (3).

$$\underset{c_t(\mathrm{WH})-x}{\mathbf{1}} + \mathrm{HOR}(\mathrm{R} = \underset{c_t(\mathrm{alc})-x}{\mathrm{CH(CH_3)_2}}, 3, 4, 5-\mathrm{Me_3C_2H_2}) \underset{x}{\rightarrow} \mathbf{7a}, \mathbf{b}, \mathbf{3a}, \mathbf{b}$$

$$K = c(\mathrm{add})/c(\mathrm{WH}) \cdot c(\mathrm{alc}) = x/(c_t(\mathrm{WH}) - x) \cdot (c_t(\mathrm{alc}) - x) \quad (8)$$

$$X(\mathrm{add}) = x/c_t(\mathrm{WH}) \quad (9)$$

$$X(WH) = 1 - X(add) \quad (10)$$

c(add) = x is calculated solving Eq. (8) and X(add) and X(WH) are calculated from Eq. (9) and (10). Then, based on Eqs. (4) and (5), δ(add) and $1/T_1$(min)(add) values were calculated.

From the determined T_1(min) values of the averaged hydride resonance and subsequently from their excess relaxation rates ΔR_1(min), the distance to the OH protons could be calculated [12,27,86,88–90]. Distances r(H···H) in [Å] can be obtained from Eq. (11) [12,27,91–95] where ν is the NMR frequency in MHz and $\Delta R_1(\min) = 1/T_1(\min)(\mathrm{add}) - 1/T_1(\min)(\mathrm{WH})$.

$$r(\mathrm{H}\cdots\mathrm{H}) = 5.817(\nu \cdot \Delta R1(\min))^{-1/6} \quad (11)$$

From van't Hoff linear regressions of $\ln K_{(\Delta\delta)}$ and $\ln K_{(\Delta R_1)}$ vs. $1/T$ the enthalpies $\Delta H_{(\Delta\delta)}$ and $\Delta H_{(\Delta R_1)}$ with errors of 8.7% and 6.9% and the entropies $\Delta S_{(\Delta\delta)}$ and $\Delta S_{(\Delta R_1)}$ with errors of 7.7% and 6.8% were determined.

4.12. Equilibrium analysis of the dihydrogen bonded adducts **3a** ($WH\cdots HOC_6H_2(CH_3)_3$) and **3b** ($W–NO\cdots HOC_6H_2(CH_3)_3$) between **1** and 3,4,5-trimethylphenol (**TMP**)

Compound **1** was dissolved in 0.5 ml of toluene-d_8 (7 mg, c_t(WH) = 0.0297 mol/L) in an NMR tube below 223 K and the chemical shifts δ(WH) and T_1(min)(WH) of the hydride ligand of **1** were determined in the temperature range of 203–243 K. Under the same conditions the chemical shifts δ(eq) and the values T_1(min)(eq) of the hydride ligand of **1** were determined for the five different solutions of 7 mg of **1** in 0.7 ml of toluene-d_8 (c_t(WH) = 0.0297 mol/L) with various concentrations of 3,4,5-trimethylphenol (c(alc) = 0.0315, 0.0591, 0.0784, 0.1099 and 0.1342 mol/L) prepared in Young tap NMR tubes. Equilibrium constants $K_{(\Delta\delta)}$ and $K_{(\Delta R_1)}$ were determined in an analogous way as for the equilibrium analysis of **1** and isopropanol. The determined enthalpies $\Delta H_{(\Delta\delta)}$ and $\Delta H_{(\Delta R_1)}$ were obtained with errors of 12.5% and 6.9%, while the entropies $\Delta S_{(\Delta\delta)}$ and $\Delta S_{(\Delta R_1)}$ were obtained with errors of 21.4% and 8.3%.

4.13. X-ray diffraction study

A single crystal of **2** was mounted on top of a glass fibre using polybutene oil as protecting agent, and immediately transferred to the diffractometer. There the crystal was cooled to 183(2) K by an Oxford cryogenic system. The determination of the unit cell parameters and the collection of intensity data were performed with an image plate detector system (Stoe IPDS diffractometer) with graphite monochromated Mo Kα radiation using the Stoe IPDS software version 2.92 (1999) [96]. A total of 167 images were exposed at a constant time of 1.50 min/image. The total exposure and read-out time was 16 h. The crystal-to-image distance was set to 50 mm (θ_{max} = 30.31°). The ϕ rotation mode was selected for the ϕ increment of 1.2° per exposure. A total of 8000 reflections with $I > 6\sigma(I)$ was selected out of the whole limiting sphere for the cell parameter refinements. A total of 26902 was collected of which 6588 were unique (R_{int} = 0.0544). The intensities were corrected from Lorentz and polarization factors and numerical absorption corrections based on 8 indexed crystal faces were also applied. The Patterson method was used to solve the crystal structures of **2** by applying the software options of the program *shelxs*-97 [97]. The structure refinements were performed with the program *shelxl*-97 [97]. The program PLATON [98] was used to check the result of the X-ray analysis and the program ORTEP [99] used to give a representation of the structure. Details of crystallographic data and refinements of complex **2** are summarized in Table 2.

Table 2
Summary of crystallographic data for complex **2**.

Compound	**2**
Empirical formula	$C_{16}H_{32}NO_3P_3W$
Formula weight (g·mol^{-1})	563.19
Temperature (K)	183(2)
Wavelength (Å)	0.71073
Crystal system, space group	Monoclinic, $P\,2_1/n$
a (Å)	11.4798(8)
b (Å)	13.9009(8)
c (Å)	15.1070(10)
α (°)	90
β (°)	107.912(8)
γ (°)	90
Volume (Å^3)	2293.9(3)
Z, density (calcd) (Mg·m^{-3})	4, 1.631
Abs coefficient (mm^{-1})	5.258
Crystal size (mm^3)	0.26 × 0.26 × 0.17
Absorption correction	Numerical
Max/min transmission	0.487/0.342
Final R_1 and wR_2 indices [$I > 2\sigma(I)$]	0.0351, 0.0707
R_1 and wR_2 indices (all data)	0.0624, 0.0734

Acknowledgment

We thank the University of Zürich and the Swiss National Science Foundation for financial support.

Appendix A. Supplementary material

CCDC 728847 contains the supplementary crystallographic data for this paper. These data can be obtained free of charge from The Cambridge Crystallographic Data Centre via www.ccdc.cam.ac.uk/data_request/cif. Supplementary data associated with this article can be found, in the online version, at doi:10.1016/j.jorganchem.2009.10.036.

References

[1] R. Custelcean, J.E. Jackson, Chem. Rev. 101 (2001) 1963.
[2] L.M. Epstein, E.S. Shubina, Coord. Chem. Rev. 231 (2002) 165.
[3] E.S. Shubina, A.N. Krylov, A.Z. Kreindlin, M.I. Rybinskaya, L.M. Epstein, J. Organomet. Chem. 465 (1994) 259.
[4] L.M. Epstein, E.S. Shubina, A.N. Krylov, A.Z. Kreindlin, M.I. Rybinskaya, J. Organomet. Chem. 447 (1993) 277.
[5] E.S. Shubina, A.N. Krylov, N.V. Belkova, L.M. Epstein, A.P. Borisov, V.D. Mahaev, J. Organomet. Chem. 493 (1995) 275.
[6] N.V. Belkova, A.V. Ionidis, L.M. Epstein, E.S. Shubina, S. Gründemann, N.S. Golubev, H.-H. Limbach, Eur. J. Inorg. Chem. (2001) 2163.
[7] D. Milstein, J.C. Calabrese, I.D. Williams, J. Am. Chem. Soc. 108 (1986) 6387.
[8] R.C. Stevence, R. Bau, D. Milstein, O. Blum, T.F. Koetzle, J. Chem. Soc., Dalton Trans. (1990) 1429.
[9] A.J. Lough, S. Park, R. Ramachandran, R.H. Morris, J. Am. Chem. Soc. 116 (1994) 8356.

[10] S. Park, R. Ramachandran, A.J. Lough, R.H. Morris, J. Chem. Soc., Chem. Commun. (1994) 2201.
[11] J.C. Lee, E. Peris, A.L. Rheingold, R.H. Crabtree, J. Am. Chem. Soc. 116 (1994) 11014.
[12] E.S. Shubina, N.V. Belkova, A.N. Krylov, E.V. Vorontsov, L.M. Epstein, D.G. Gusev, M. Niedermann, H. Berke, J. Am. Chem. Soc. 118 (1996) 1105.
[13] N.V. Belkova, E.S. Shubina, A.V. Ionidis, L.M. Epstein, H. Jacobsen, A. Messmer, H. Berke, Inorg. Chem. 36 (1997) 1522.
[14] E.S. Shubina, N.V. Belkova, E.V. Bakhmutova, L.N. Saitkulova, A.V. Ionidis, L.M. Epstein, Russ. Chem. Bull. 47 (1999) 817.
[15] N.V. Belkova, E.S. Shubina, E.I. Gutsul, L.M. Epstein, I.L. Eremenko, S.E. Nefedov, J. Organomet. Chem. 610 (2000) 58.
[16] L.M. Epstein, N.V. Shubina, E.V. Bakhmutova, L.N. Saitkulova, V.I. Bakhmutov, A.L. Chistyakov, I.V. Stankevich, Inorg. Chem. 37 (1998) 3013.
[17] L.A. Vinogradova, A.Z. Kreindlin, L.A. Leites, I.T. Chizevskii, E.S. Shubina, L.M. Epstein, Metalloorg. Khim. 3 (1990) 1192.
[18] S.G. Kazarian, P.A. Hamley, M. Poliakoff, J. Am. Chem. Soc. 115 (1993) 9069.
[19] S.G. Kazarian, P.A. Hamley, M. Poliakoff, J. Chem. Soc., Chem. Commun. (1992) 995.
[20] M. Poliakoff, S.M. Howdle, S.G. Kazarian, Angew. Chem., Int. Ed. Engl. 34 (1995) 1275.
[21] E.S. Shubina, N.V. Belkova, L.M. Epstein, J. Organomet. Chem. 536 (1997) 17.
[22] R.H. Crabtree, J. Organomet. Chem. 557 (1998) 111.
[23] N.V. Belkova, M. Besora, L.M. Epstein, A. Liedós, F. Maseras, E.S. Shubina, J. Am. Chem. Soc. 125 (2003) 7715.
[24] N.V. Belkova, P.O. Revin, L.M. Epstein, E.V. Vorontsov, V.I. Bakhmutov, E.S. Shubina, E. Collange, R. Poli, J. Am. Chem. Soc. 125 (2003) 11106.
[25] E.I. Gutsul, N.V. Belkova, M.S. Sverdlov, L.M. Epstein, E.S. Shubina, V.I. Bakhmutov, T.N. Gribanova, R.M. Minyaev, C. Bianchini, M. Peruzzini, F. Zanobini, Chem. Eur. J. 9 (2003) 2219.
[26] E.V. Bakhmutova, V.I. Bakhmutov, N.V. Belkova, M. Besora, L.M. Epstein, A. Liedós, G.I. Nikonov, E.S. Shubina, J. Tomàs, E.V. Vorontsov, Chem. Eur. J. 10 (2004) 661.
[27] A. Messmer, H. Jacobsen, H. Berke, Chem. Eur. J. 5 (1999) 3341.
[28] E.S. Shubina, A.N. Krylov, D.V. Muratov, A.A. Fil'chikov, L.M. Epstein, Russ. Chem. Bull. 42 (1993) 1919.
[29] L.M. Epstein, N.V. Belkova, E.S. Shubina, in: M. Peruzzini, R. Poli, (Eds.), Advances in Hydride Chemistry, Elsevier, 2001, p. 391.
[30] E. Peris, J.C. Lee, J.R. Rambo, O. Eisenstein, R.H. Crabtree, J. Am. Chem. Soc. 117 (1995) 3485.
[31] J.C. Lee, A. Rheingold, B. Muller, P.S. Pregosin, R.H. Crabtree, J. Chem. Soc., Chem. Commun. (1994) 1021.
[32] K. Abdur-Rashid, T.P. Fong, B. Greaves, D.G. Gusev, J.G. Hinman, S.E. Landau, A.J. Lough, R.H. Morris, J. Am. Chem. Soc. 122 (2000) 9155.
[33] H.S. Chu, C.P. Lau, K.Y. Wong, Organometallics 17 (1998) 2768.
[34] Y. Musashi, S. Sakaki, J. Am. Chem. Soc. 122 (2000) 3867.
[35] A. Caballero, F.A. Jalón, B.R. Manzano, Chem. Commun. (1998) 1879.
[36] W. Yao, R.H. Crabtree, Inorg. Chem. 35 (1996) 3007.
[37] S. Aime, R. Gobetto, E. Valls, Organometallics 16 (1997) 5140.
[38] J. Wessel, J.C. Lee, E. Peris, G.P.A. Yap, J.B. Fortin, J.S. Ricci, G. Sini, A. Albinati, T.F. Koetzle, O. Eisenstein, A.L. Rheingold, R.H. Crabtree, Angew. Chem., Int. Ed. Engl. 34 (1995) 2507.
[39] G. Sini, O. Eisenstein, W. Yao, R.H. Crabtree, Inorg. Chim. Acta 280 (1998) 26.
[40] B.P. Patel, J. Wessel, W. Yao, J.C. Lee, E. Peris, T.F. Koetzle, G.P.A. Yap, J.B. Fortin, J.S. Ricci, G. Sini, A. Albinati, O. Eisenstein, A.L. Rheingold, R.H. Crabtree, New J. Chem. 21 (1997) 413.
[41] B.P. Patel, W. Yao, G.P.A. Yap, A.L. Rheingold, R.H. Crabtree, Chem. Commun. 8 (1996) 991.
[42] G.J. Kubas, Acc. Chem. Res. 21 (1988) 120.
[43] P.G. Jessop, R.H. Morris, Coord. Chem. Rev. 121 (1992) 155.
[44] F. Maseras, A. Lledós, E. Clot, O. Eisenstein, Chem. Rev. 100 (2000) 601.
[45] L.M. Epstein, E.S. Shubina, Ver. Bunsenges. Phys. Chem. 102 (1998) 359.
[46] E.S. Shubina, N.V. Belkova, E.V. Bakhumotova, L.N. Saitkulova, A.V. Ionidis, L.M. Epstein, Izv. Akad. Nauk, ser. Khim. (1999) 846.
[47] L.M. Epstein, A.N. Krylov, E.S. Shubina, J. Mol. Struct. 322 (1994) 345.
[48] S.G. Kazarian, P.A. Hamley, M. Poliakoff, J. Am. Chem. Soc 115 (1993) 9069.
[49] W.T. Klooster, T.F. Koetzle, P.E.M. Siegbahn, T.B. Richardson, R.H. Crabtree, J. Am. Chem. Soc. 121 (1999) 6337.
[50] E.S. Shubina, N.V. Belkova, E.V. Bakhmutova, E.V. Vorontsov, V.I. Bakhmutov, A.V. Ionidis, C. Bianchini, L. Marvelli, M. Peruzzini, L.M. Epstein, Inorg. Chim. Acta 280 (1998) 302.
[51] V.I. Bakhmutov, E.V. Bakhmutova, N.V. Belkova, C. Bianchini, L.M. Epstein, M. Peruzzini, E.S. Shubina, E.V. Vorontsov, F. Zanobini, Can. J. Chem. 79 (2001) 475.
[52] A.A.H. van der Zeijden, H.W. Bosch, H. Berke, Organometallics 11 (1992) 2051.
[53] A.A.H. van der Zeijden, V. Shklover, H. Berke, Inorg. Chem. 30 (1991) 4393.
[54] A.A.H. van der Zeijden, D. Veghini, H. Berke, Inorg. Chem. 31 (1992) 5106.
[55] A.A.H. van der Zeijden, H. Berke, Helv. Chim. Acta 75 (1992) 513.
[56] A.A.H. van der Zeijden, H.W. Bosch, H. Berke, Organometallics 11 (1992) 563.
[57] H. Berke, P. Burger, Comments Inorg. Chem. 16 (1994) 279.
[58] D. Nietlispach, D. Veghini, H. Berke, Helv. Chim. Acta 77 (1994) 2197.
[59] F. Bäth, Ph.D. Thesis, University of Zürich, 1998.
[60] F. Furno, T. Fox, H.W. Schmalle, H. Berke, Organometallics 19 (2000) 3620.
[61] H. Jacobsen, H.W. Schmalle, A. Messmer, H. Berke, Inorg. Chim. Acta 306 (2000) 153.
[62] F.P. Liang, H. Jacobsen, H.W. Schmalle, T. Fox, H. Berke, Organometallics 19 (2000) 1950.
[63] F. Furno, T. Fox, M. Alfonso, H. Berke, Eur. J. Inorg. Chem. (2001) 1559.
[64] J. Höck, H. Jacobsen, H.W. Schmalle, G.R.J. Artus, T. Fox, J.I. Amor, F. Bäth, H. Berke, Organometallics 20 (2001) 1533.
[65] A. Llamazares, H.W. Schmalle, H. Berke, Organometallics 20 (2001) 5277.
[66] X.Y. Liu, S. Bouherour, H. Jacobsen, H.W. Schmalle, H. Berke, Inorg. Chim. Acta 330 (2002) 250.
[67] F.P. Liang, H.W. Schmalle, T. Fox, H. Berke, Organometallics 22 (2003) 3382.
[68] F.P. Liang, H.W. Schmalle, H. Berke, Inorg. Chem. 43 (2004) 993.
[69] Z. Chen, H.W. Schmalle, T. Fox, H. Berke, J. Chem. Soc., Dalton Trans. (2005) 580.
[70] E. Bannwart, H. Jacobsen, F. Furno, H. Berke, Organometallics 19 (2000) 3605.
[71] D. Nietlispach, H.W. Bosch, H. Berke, Chem. Ber. 127 (1994) 2403.
[72] H. Jacobsen, K. Heinze, A. Llamazares, H.W. Schmalle, G. Artus, H. Berke, J. Chem. Soc., Dalton Trans. (1999) 1717.
[73] D.G. Gusev, A. Llamazares, G. Artus, H. Jacobsen, H. Berke, Organometallics 18 (1999) 75.
[74] H.-U. Hund, U. Ruppli, H. Berke, Helv. Chim. Acta 76 (1993) 963.
[75] D.G. Gusev, D. Nietlispach, I.L. Eremenko, H. Berke, Inorg. Chem. 32 (1993) 3628.
[76] Z. Yin, Ph.D. Thesis, University of Zürich, 2005.
[77] J. Höck, T. Fox, H.W. Schmalle, H. Berke, Chimia 53 (1999) 350.
[78] Z. Chen, Ph.D. Thesis, University of Zürich, 2004.
[79] A. Messmer, Ph.D. Thesis, University of Zürich, 1999.
[80] A.A.H. van der Zeijden, C. Sontag, H.W. Bosch, V. Shklover, H. Berke, D. Nanz, W. von Philipsborn, Helv. Chim. Acta 74 (1991) 1194.
[81] E.M. Arnett, L. Joris, E. Mitchell, T.S.S.R. Murty, T.M. Gorrie, P.V.R. Schleyer, J. Am. Chem. Soc. 92 (1970) 2365.
[82] M.C.S. Lopes, H.W. Thompson, Spectrochim. Acta 24A (1968) 1367.
[83] A.A. Frost, R.G. Pearson, in: Kinetics and Mechanism, second ed., John Wiley & Sons, New York, London, 1961.
[84] (a) Win-IR, FTS 25 and FTS 40 Spectrometer Manuel, Technical Publications Bio-Rad Labaratories, Cambridge.;
(b) MERLIN, Merlin Reference Manuel, Technical Publications Bio-Rad Laboratories, Cambridge.
[85] (a) D.G. Cameron, D.J. Moffatt, J. Test. Evalut. 2 (1984) 78;
(b) W.-J. Yang, P. Griffiths, Comput. Enhanced Spectrosc. 3 (1983) 157;
(c) J.K. Kauppinen, D.J. Moffat, H.H. Mantsch, D.G. Cameron, Appl. Spectrosc. 3 (1981) 271.
[86] A. Abragam, The Principles of Nuclear Magnetism, Oxford University Press, Oxford, 1973.
[87] W.H. Press, B.P. Flannery, S.A. Teukolsky, W.T. Vetterling, Numerical Recipes, Cambridge University Press, Cambridge, 1986 (1988 reprint, Chapter 14.4).
[88] P.J. Desrosiers, L. Cai, Z. Lin, R. Richards, J. Halpern, J. Am. Chem. Soc. 113 (1991) 4173.
[89] R.H. Morris, Can. J. Chem. 74 (1996) 1907.
[90] D.G. Hamilton, R.H. Crabtree, J. Am. Chem. Soc. 110 (1988) 4126.
[91] R. Cammack, Nature 373 (1995) 556.
[92] R.T. Hembre, S. McQueen, J. Am. Chem. Soc. 116 (1994) 2141.
[93] K.-J. Haack, S. Hashiguchi, A. Fujii, T. Ikariya, R. Noyori, Angew. Chem., Int. Ed. Engl. 36 (1997) 285.
[94] J.-S. Song, D.J. Szalda, R.M. Bullock, C.J.C. Lawrie, M.A. Rodkin, J.R. Norton, Angew. Chem. 104 (1992) 1280.
[95] J.-S. Song, D.J. Szalda, R.M. Bullock, C.J.C. Lawrie, M.A. Rodkin, J.R. Norton, Angew. Chem., Int. Ed. Engl. 31 (1992) 1233.
[96] STOE-IPDS Software package. STOE & Cie, Darmstadt, Germany.
[97] G.M. Sheldrick, Acta Crystallogr., Sect. A64 (2008) 112.
[98] A.L. Spek, J. Appl. Crystallogr. 36 (2003) 7.
[99] L.J. Farrugia, J. Appl. Crystallogr. 30 (1997) 565.